THE JOURNAL OF COMPARATIVE NEUROLOGY 418:423–440 (2000)

Changes in Efferent and Afferent Connectivity in Rats With Induced Cerebrocortical Microgyria

GLENN D. ROSEN,[1,2]* DEBORAH BURSTEIN,[3] AND ALBERT M. GALABURDA[1,2]
[1]Dyslexia Research Laboratory and Charles A. Dana Research Institute, Division of Behavioral Neurology, Department of Neurology, Beth Israel Deaconess Medical Center, Boston Massachusetts 02215
[2]Harvard Medical School, Boston, Massachusetts 02115
[3]Department of Radiology, Beth Israel Deaconess Medical Center, Boston Massachusetts 02215

ABSTRACT

Freezing injury to the cortical plate at postnatal day (P) 1 initiates a cascade of events that ultimately result in a focal neocortical malformation resembling human 4-layered microgyria. This malformation has been associated with widespread changes in neocortical and thalamic architecture and physiology. It was hypothesized that at least some of these alterations could result from connectional reorganization following early injury. The current experiment was designed to delineate the efferent and afferent connections between the cerebral hemispheres and between the cortex and thalamus of rats with induced cerebrocortical microgyria. Microgyria were induced in the parietal cortex of rats by freezing injury on postnatal day 1. In adulthood, injections of biotinylated dextran amine were made either in the microgyric cortex, in homologous regions of the opposite hemisphere, or in ipsilateral ventrobasal complex of the thalamus. Appropriately directed connections to homotopic areas were seen in some but not all microgyric rats. In addition, heterotopic projections to frontal and secondary sensorimotor cortices were noted. Projections from homotopic regions in the hemisphere opposite to the malformation terminated most often in the medial portions of the microgyrus or avoided it entirely. There were almost no thalamocortical or corticothalamic projections between the ventrobasal complex and the microgyrus itself, although a dense plexus of thalamocortical fibers was often noted at the border between the malformed and normal cortex. These connectional changes may help explain disturbances in architecture, physiology, and behavior associated with these focal malformations. J. Comp. Neurol. 418: 423–440, 2000.

Indexing terms: brain malformation; cerebral cortex; thalamus; parietal cortex; rat; microgyria

Damage to the brain during development affects typical patterns of neuronal connectivity. In hamsters, unilateral neonatal lesions of the superior colliculus result in restructuring of afferent connections (Finlay et al., 1979; Schneider, 1979, 1981). Specifically, these lesions cause optic fibers to cross the midline where they compete successfully for available terminal space in the intact superior colliculus. In monkeys, prenatal unilateral removal of portions of the frontal cortex results in significant displacement of callosal connections (Goldman and Galkin, 1978; Goldman-Rakic and Rakic, 1984).

However, not all abnormal events occurring during brain development affect the eventual patterns of connectivity. The reeler mouse cerebral cortex, which is characterized by inversion of the cortex resulting from a disturbance in neuronal migration (D'Arcangelo et al., 1995), has efferent connections that arise from appropriate neuronal types irrespective of their laminar location (Caviness, 1976; Caviness and Yorke, 1976; Caviness, 1982; Caviness and Frost, 1983; Goffinet et al., 1984; Frost et al.,

Grant sponsor: National Institutes of Health and US Public Health Service; Grant number: HD20806.

*Correspondence to: Glenn D. Rosen, Department of Neurology, Beth Israel Deaconess Medical Center, 330 Brookline Avenue, Boston, MA 02215. E-mail: grosen@caregroup.harvard.edu

Received 28 May 1999; Revised 21 November 1999; Accepted 23 November 1999

1986). Thus, the cells of origin of callosal projections in both cases are medium-sized pyramids located in the superficial layers of normal cortex and in the deepest layer of reeler cortex.

More recently, a mutant strain of rats that develops a telencephalic internal structural heterotopia (*tish*) has been investigated (Lee et al., 1997). These rats form an ectopic collection of neurons below the cortical plate, which appears to be neocortical in origin and morphology (Lee et al., 1998). These animals are susceptible to spontaneous seizures, and the *tish* animals are proposed to be a model for human double cortex. Interestingly, this heterotopic cortex appears to have relatively normal subcortical sensory and motor connections, as determined by anterograde and retrograde labeling techniques (Schottler et al., 1998). Similarly, rats injected prenatally with methylazoxymethanol (MAM) have microcephalic brains and ectopic neurons in the subcortical white matter and CA1 of the hippocampus (Singh, 1977; Johnston and Coyle, 1979; Dambska et al., 1982). These rats have a decreased seizure threshold (Baraban and Schwartzkroin, 1996; Chevassus-au-Louis et al., 1998a), and changes in glutamate receptors (Rafiki et al., 1998). The ectopic neurons in CA1 appear to be well integrated electrophysiologically and connectionally into both the cortical (reflecting the neuron's origin) and hippocampal (reflecting their location) circuitry, and may serve as a functional bridge between hippocampus and cortex (Chevassus-Au-Louis et al., 1998b,c).

It would be reasonable to conclude, then, that at least some disorders affecting neuronal migration have little effect on the patterns of inherent connectivity of the brain. There is evidence, however, that neuropathological events occurring during the period of neuronal migration to the cerebral cortex could have profound effects *both* on the eventual laminar disposition of neurons and on the patterns of intrinsic connectivity. For example, injection of ibotenic acid into the visual cortex of cats on postnatal days 2 and 3 causes death primarily of infragranular neurons and the subsequent formation of microgyric-like cortex (Innocenti and Berbel, 1991a). Furthermore, this microgyric cortex continues to receive projections from auditory areas AI and AII — projections that are normally eliminated during development (Innocenti and Berbel, 1991b). Cerebral hypoxia induced by neonatal carotid ligation in cats results in a marked increase in efferent projections from visual cortex to the opposite hemisphere (Miller et al., 1993b). Finally, disturbed interhemispheric connectivity has been associated with a spontaneously occurring microgyrus in the rat (Rosen et al., 1989). Specifically, four-layered cortex was seen surrounding a microsulcus consisting of infolded, fused molecular layers and containing ectopic neurons. Callosal termination within this microgyrus did not show the normal pattern of lamination, and instead there was a band of dense axonal termination with projection-rich bridges to deeper cortical layers (Rosen et al., 1989).

As described by Dvorák and colleagues (Dvorák and Feit, 1977; Dvorák et al., 1978), regions of focal cerebrocortical microgyria are reliably induced in neonatal rat neocortex by placement of a freezing probe on the skulls of newborn rats (Humphreys et al., 1991; Rosen et al., 1992a). The formation of microgyria is thought to be the result of basic brain repair mechanisms occurring during the end of the period of neuronal migration (Suzuki and Choi, 1991; Rosen et al., 1992a). Adult rats with these induced malformations exhibit specific behavioral findings (Fitch et al., 1994, 1997; Rosen et al., 1995b), and the brains of these animals show physiologic (Luhmann and Raabe, 1996; Jacobs et al., 1997; Luhmann et al., 1997, 1998) and anatomic changes (Herman et al., 1997; Rosen et al., 1998; Zilles et al., 1998; Rosen et al., 1999) that have been hypothesized to be the result of changes in connectivity associated with the malformation (Rosen et al., 1998, 1999). In the present study, we investigated directly the effect of injury to the cortical plate on patterns of callosal, corticothalamic, and thalamocortical connections.

METHODS

All protocols for the experiments detailed below were approved by the IACUC of Beth Israel Deaconess Medical Center.

Protocol

A series of three experiments were performed on adult rats that had received freezing lesions to the parietal cortex neonatally: Experiment 1 was designed to determine the efferent and afferent callosal projections of microgyric cortex following injections of a neuronal tracer in the microgyric region. Experiment 2 examined the pattern of callosal projections following injection of a neuronal tracer into homologous regions of cortex. Experiment 3 was designed to trace the afferent and efferent connections of the ventrobasal thalamus (the main source of efferent projections to, and target of afferent projections from, parietal cortex).

Pregnant Wistar rats were obtained from Charles River Laboratories (Wilmington, MA). On the day after birth (P1), pups were randomly assigned to receive unilateral freezing injuries to the parietal cortex (regions Par1, HL, and FL from Zilles, 1985) or to a sham condition. For Experiments 1 and 3, the freezing injury (or sham surgery) was in the right hemisphere, for Experiment 2, either hemisphere. At P70, the brains of animals from Experiment 3 were imaged in vivo using magnetic resonance imaging (MRI) to confirm the location of the microgyrus. At P100 pairs of microgyric and control subjects were given stereotaxically placed injections of 10% biotinylated dextran amine (BDA) as described below. Subjects were killed 4–7 days later, and their brains processed for visualization of the neuronal tracer, and their patterns of connections analyzed under light and darkfield illumination.

Induction of microgyria

Microgyria were induced based on a modification of a technique by Dvorák and colleagues (Dvorák and Feit, 1977; Dvorák et al., 1978), and reported in detail elsewhere (Humphreys et al., 1991; Rosen et al., 1992a). Pups were anesthetized with hypothermia, and a small incision was made in the anteroposterior plane of the skin over midline, exposing the skull. A cooled (−70°C) 2 mm diameter stainless steel probe was placed on the skull of lesion subjects over the cerebral hemisphere for 5 seconds. The probe, targeted at the presumptive parietal cortex, was placed 1 mm caudal to bregma and 2 mm lateral of the sagittal suture. Animals receiving sham surgery were treated identically to those receiving freezing injury except that the probe was maintained at room temperature. These parameters (probe size, time of freezing lesion, location, and temperature) were chosen because previous research had shown them to yield malformations of consistent size and relatively predictable location (Rosen et

al., 1992a,b, 1994, 1995b, 1996, 1997, 1998, 1999). The skin was quickly sutured, and subjects were marked with a unique pattern of ink injection to the footpads, warmed under a lamp, and returned to the mother. On P21, litters were weaned and experimental subjects were housed with their controls.

MRI

Subjects in Experiment 3 were anesthetized (87% Ketamine/13% Xylazine; 100 mg/kg i.p.) and placed in a 4.7 T 30 cm bore MRI instrument (Bruker Instruments, Billerica, MA) and their heads imaged as described previously (Rosen and Burstein, 1997). The general protocol was to first acquire a scout image in the sagittal plane from which a multislice coronal data set was obtained. The sagittal scout was obtained with a gradient echo sequence, with TR/TE = 500/25 ms, a field of view (FOV) of 4 cm with a 128 matrix (in plane resolution of 312 μm), and a section thickness of 1 mm. The multislice coronal data set was chosen to cover the region of interest. Twelve contiguous slices were obtained with the parameters TR/TE = 500/10 or 300/20, a FOV of 3.2 cm, with a 128 matrix (in plane resolution of 250 μm), and a section thickness of 0.5 mm. Acquisitions were averaged for a total imaging time of 20–30 minutes.

Biotinylated dextran amine (BDA) injections

For all experiments, injections of 0.05 μl 10% BDA (Molecular Probes, Eugene, Oregon) were placed stereotaxically. All animals were injected with a Hamilton 7001 syringe (Hamilton Company, Reno, NV). Description of the injection protocols for each of the experiments are described below.

Experiment 1. Animals were anesthetized (87% Ketamine/13% Xylazine; 100/mg kg i.p.) and placed in a stereotaxic apparatus (David Kopf Instruments, Tujunga, CA). The skull of the lesioned animal was exposed following a midline incision and the mediolateral (M-L), rostrocaudal (R-C), and dorsoventral (D-V) coordinates of Bregma recorded. A bone flap was removed from the skull over the right hemisphere and enlarged with rongeurs. The location of the microgyrus was located and the M-L and R-C coordinates noted and their values subtracted from those of Bregma. The tip of the syringe was then placed on the pial surface and the D-V coordinate recorded. The syringe was then lowered 0.6 mm into the cortex and an injection was made. The syringe was left in place for 5 minutes before being removed. Hemostasis (if necessary) was obtained with Gelfoam before suturing.

Controls were prepared identically to the lesioned subjects as described above with their injections placed using the M-L and R-C differentials as determined from their matched littermates. The unique D-V coordinate was determined for each animal. Injections proceeded as above.

Experiment 2. Animals were anesthetized and the coordinates of the microgyrus noted as described above. An additional bone flap was made over the opposite hemisphere and the syringe moved to the recorded R-C differential and the reversed M-L differential coordinate. Injections proceeded as described above.

Controls were prepared identically to the lesioned subjects as described above with their injections placed in the left hemisphere using the M-L and R-C differentials as determined from their matched littermates.

Experiment 3. Both lesioned and control rats were anesthetized and the coordinates of Bregma located as above. The syringe was moved to coordinates −3.3 R-C and −2.5 M-L (Paxinos and Watson, 1986). A small burr hole was made with a drill and the syringe inserted 6.5 mm D-V, and BDA was injected as described above.

Histology

Subjects were killed 4–7 days following stereotaxic surgery. They were anesthetized (87% Ketamine/13% Xylazine; 100/mg kg i.p.) and were transcardially perfused with 0.9% saline and 4% paraformaldehyde (pH 7.4). The brains were removed and placed in the fixative for 24 hours. The brains were then cryoprotected by placement in a 10% buffered sucrose (pH 7.4) solution for 24 hours before being serially cut in the coronal plane frozen on a sliding microtome at 40 μm. A series of every tenth section was mounted on subbed (chromium potassium sulfate/gelatin) slides, stained with Thionin for Nissl substance, and coverslipped with Permount. Adjacent series were reacted for visualization of BDA (see below) with one series being counterstained with methyl green and the other not.

BDA histochemistry

Free floating sections were washed in PBS (pH 7.4) and incubated with avidin-biotin peroxidase complex (Vector Laboratories, Burlington, CA) at a concentration of 1 μl/ml in PBS for 1–1.5 hour at room temperature. This was followed by several washes of PBS and the sections were then incubated in freshly prepared solutions of 0.05% nickel enhanced diaminobenzidine tetrahydrochloride (DAB). The sections were rinsed and mounted on subbed slides, counterstained with methyl-green/alcian blue, and coverslipped with Permount.

Analysis

All material was analyzed under brightfield and darkfield microscopy.

Figure preparation

Brightfield and darkfield photomicrographs were taken from a Zeiss Axiophot microscope (Carl Zeiss, Inc., Thornwood, NY) on Ektachrome 160 (Kodak, Rochester, NY) and then digitally scanned using a Nikon LS-1000 slide scanner (Nikon Inc., Melville, NY) interfaced to Power Macintosh 7600/120 (Apple Computer, Cupertino, CA). Final photomontages (see Figs. 1,2, 5, 7–10) were prepared using Adobe PhotoShop (Adobe Systems Inc., San Jose, CA) and Canvas (Deneba Corporation, Miami, FL). The images were adjusted for brightness and contrast but were not manipulated in any other way. Drawings (see Figs. 3, 4, 6) were made by first compositing digital images taken under brightfield and darkfield illumination using a Sony CCD AVC-D7 camera (Sony Corporation, New York, NY), and then importing the composite image into Canvas where labeled cells and fibers were traced. There was no digital manipulation of these images other than scaling for image alignment. Drawing of thalamic injection sites (see Figs. 8, 10) were made by first drawing borders from stereotaxic atlas (Paxinos and Watson, 1986), and then scaling digital images from actual injection sites over these drawings and tracing the border of the injection site.

RESULTS

Histology

All subjects receiving the freezing lesion to the cortical plate in the neonatal period exhibited focal cortical mal-

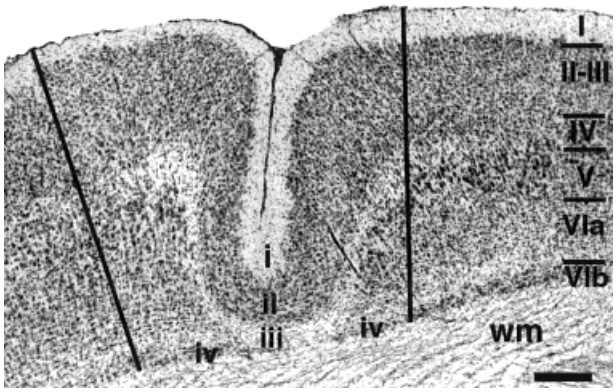

Fig. 1. Low-power photomicrograph of a typical region of induced microgyria in Par1. In comparison to the adjacent undamaged cortex (right) with six layers, microgyric cortex has four layers. Layer i is contiguous with the molecular layer of the undamaged cortex and fuses to form a microsulcus (arrow). Layer ii is contiguous with layers II and III of undamaged cortex but is unlaminated. Layer iii (*lamina dissecans*) is a glial scar that is the remnant of the original injury. Layer iv is contiguous with layer VI b of intact cortex. Solid lines show the medial and lateral borders of the microgyric area. Scale bar = 200 μm. wm, white matter.

formations resembling 4-layered microgyria, and their appearance was identical to that reported in previous work (Fig. 1). There were no differences between males and females in either the extent of the malformation, or in the patterns of connections. As expected, animals exposed to sham surgery showed no cerebral malformation.

Experiment 1: injections into microgyria

A list of all successful injections for this experiment and a summary of the results can be found in Table 1. In all controls (N=9), injections of BDA into the parietal cortices yielded patterns of afferent and efferent projections similar to those reported in the literature. Specifically, the largest component of callosal projections were to homologous neocortex. However, efferent projections were not limited to homologous regions. For example, efferent projections from Par1 were seen in HL and FL regions and occasionally in Par2 in 33% of the cases. These heterotopic projections, when present, were neither as dense nor as extensive as the homologous projections (Figs. 2–4).

In experimental animals (N=7) injections of BDA into microgyria most often revealed homologous projections, but, in contrast to controls, these projections were less dense and at times even absent (Fig. 3). Whether homotopic projections were or were not present, projections to hetereologous regions were noted in all but one case. Most frequent among these were projections laterally into Par2 and medially in the frontal cortex (Figs. 2, 4).

Experiment 2: injections into homologous cortex

A list of all successful injections for this experiment and a summary of the results can be found in Table 2. As expected, injections of BDA into the parietal cortices of controls (N=5) yielded patterns of afferent and efferent callosal projections similar to those reported in the literature, and were identical to those seen in the controls of Experiment 1. In contrast, the distribution of afferent and efferent callosal projections was less stereotyped following injections in cortex homologous to that containing microgyria (N=6). When efferent projections from the injection site innervated the microgyrus, they were overwhelmingly found in the medial portion of the malformation (Figs. 5A–C, 6). When terminals were found in the lateral portion of the microgyrus, they were far less dense than those in the medial. In one case, afferents to the microgyric hemisphere were seen to bypass the microgyrus altogether and innervate instead areas both medial and lateral to it (Fig. 5D–F).

Experiment 3: injections into ventrobasal thalamus

Although lesions were meant to placed in the parietal cortex, previous experience indicated that the malformation could sometimes be found in other architectonic regions (e.g., Rosen et al., 1999). Imaging the brains using MRI enabled confirmation of lesion locations (Fig. 7). Injections of tracers were not performed in cases where the lesion fell outside of the expected location (n=4). A list of

TABLE 1. List of Subjects and Summary of Results of Experiment 1: Injection of Tracer Into Microgyria[1]

Subject/sex	Condition	Micogyria location	Ipsilateral injection site	Contralateral projections	
				Location	Comments
3210/F	MG	Par1, HL, FL	Par1, HL, FL	Lateral Par1, Par2	Few homologous projections.
3217/M	Sham	—	Par1, HL, FL	Par1, HL, FL	Homologous projections.
3223/F	Sham	—	Par1, HL	Par1, HL	Dense homologous projections.
3224/F	MG	Fr1, HL, FL, Par1, Oc	Par1	Par1, Par2, Gu	Homologous and heterologous projections.
3226/M	MG	Par1	Par1	Par1, Par2, Gu	Homologous and heterologous projections.
3227/M	Sham	—	Par1	Par1, HL	Dense Par1, no lateral projections.
3403/M	MG	Par1, HL, Oc	Par1, FL	Fr1, FL, Par1, Par2	Mostly heterologous projections.
3404/M	Sham	—	Par1	Par1	Only homologous projections.
3407/M	MG	Par1, FL	Par1, FL	Par1, FL	Only homologous projections.
3408/M	Sham	—	Par1	Par1	Only homologous projections.
3410/M	Sham	—	HL, FL	HL, FL, Par1	Mostly homologous projections, some very lateral Par1.
3420/F	MG	Fr, HL, FL	Fr, HL, FL	Fr1, Par1, Par2	Retrograde cells in Fr1, HL, Par1, Par2. Fibers mostly in Fr 1.
3421/F	Sham	—	Fr, HL, FL	Fr1, HL, FL, Par1	Homologous projections.
3423/F	Sham	—	Par1, FL	Par1	Homologous projections.
3424/F	MG	Par1	FL	Par1, Par2	Few homologous projections, Dense heterologous projections.
3425/F	Sham	—	FL	FL, Par1, Par2	Very dense homologous projections, some heterologous projections.

[1]MG, microgyria; FL, forelimb area; Fr, frontal cortex; Gu, gustatory cortex; HL, hindlimb area; Oc, occipital cortex; Par1 and Par2, primary and secondary somatosensory cortices. Locations after Zilles (1985).

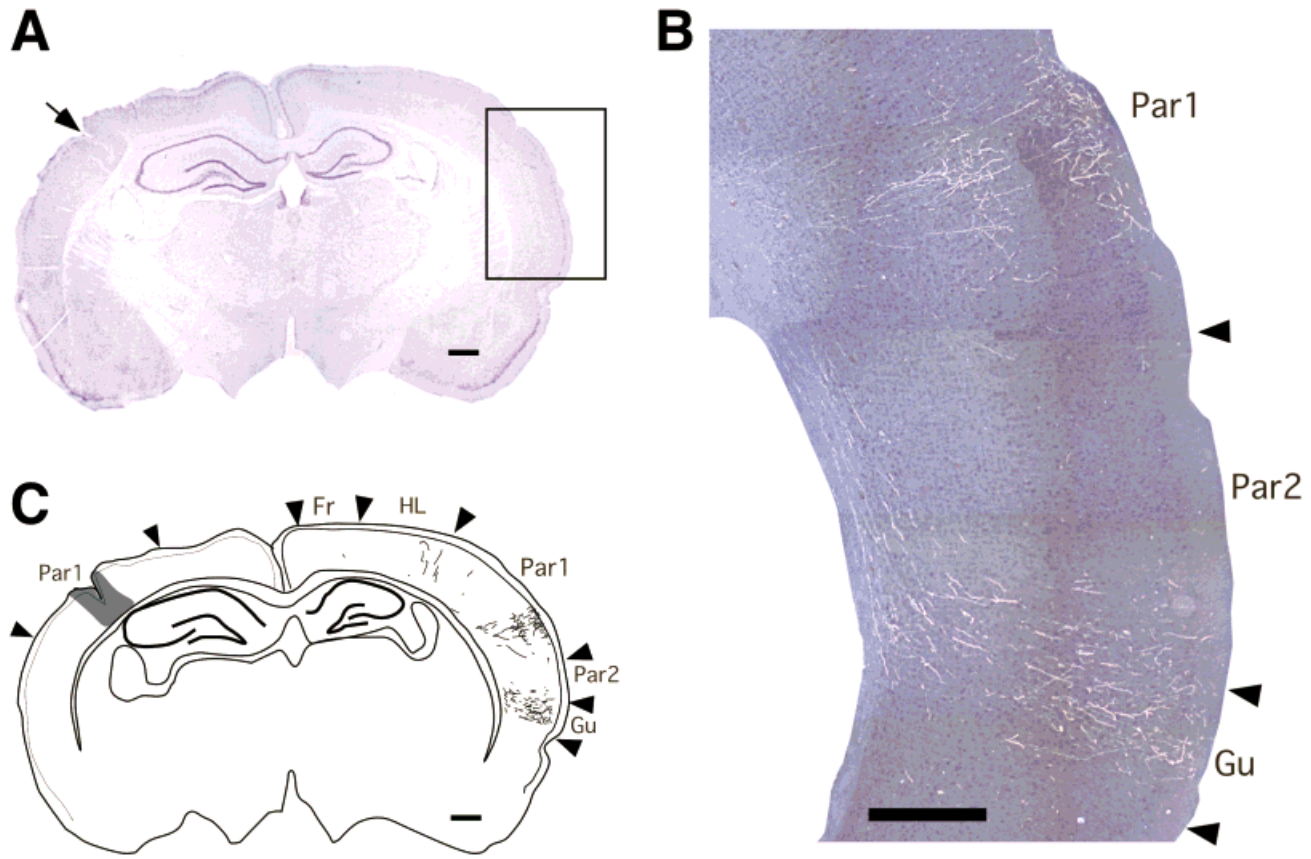

Fig. 2. Efferent callosal projections from microgyria. **A:** Photomontage of Nissl stain of Subject 3224 showing microgyria (arrow) in Par1. Box is area of magnification for **B**. See **C** for injection site. B: High-power darkfield photomontage of BDA-stained section adjacent to that in A showing efferent callosal fibers from microgyric injection site. Fibers are located in the homotopic region (Par1) and in heterotopic regions (Par2). C: Tracing of callosal projections from microgyric injection site (dark gray). Fr, Frontal cortex (including Fr1, Fr2, and Fr3); HL, Hindlimb region of parietal cortex; Par1, Primary parietal cortex; Par2, Secondary parietal cortex; Gu, Gustatory cortex. After Zilles (1985). Scale bars = 800 μm in A,C; 500 μm in B.

all successful injections for this experiment and a summary of the results can be found in Table 3.

In control subjects (N=9), injections using the stereotaxic coordinates described above revealed a large reciprocal projection field between the ventrobasal complex of the thalamus and the central and lateral portions of Par1 (Figs. 8–10). By contrast, injections into the ventrobasal complex of microgyric rats (N=19) yielded a pattern of reciprocal projections notable for a virtual absence of terminations in the region of the malformation (Figs. 8–10). At the border of the microgyrus, there was a dense plexus of fibers in the supragranular layers noted in eight cases. Similar patches of termination were seen in control subjects in association with barrel fields, but in the case of the controls, they were not as dense as in the experimental subjects.

DISCUSSION

Injections of neuronal tracers in rats with induced focal malformations of the neocortex revealed differences in neuronal connectivity when compared to unlesioned rats. In terms of callosal efferent connectivity from the malformation, we found an increase in density of heterotopic projections, and in some cases total absence of normal homotopic innervation. Callosal projections from homotopic regions of the undamaged hemisphere tended to innervate the medial portion of the microgyrus or avoided the microgyrus altogether. These changes in callosal connectivity are unlikely to be the result of labeling of en passant fibers, since these heterotopic connections are not often seen in control animals, and when present are not

Fig. 3. (Overleaf) Tracing of darkfield photomontages of injection into a microgyrus located in the FL region of the right hemisphere of Subject 3424 (dark gray), illustrating retrograde and anterograde callosal connections. Retrogradely labeled cells are represented as filled circles, and anterogradely labeled fibers are traced. Dense patches of projections are represented by light gray-filled regions. Patterns of projections to the left hemisphere are notable for an absence of the normal homotopic projections to FL as seen in the matched control, Subject 3425 (**A–C**). In the microgyric case, the densest projections are located in Par1 (**B–D**) and are far less dense than those in the control. For all figures, architectonic boundaries were determined primarily by topography. In the case of the distorted architecture of the malformation, microscopic architectonic parcellation of adjacent intact cortex confirmed the location. Fr, Frontal cortex (including Fr1, Fr2, and Fr3); FL, Forelimb area of parietal cortex; HL, Hindlimb region of parietal cortex; Par1, Primary parietal cortex; Par2, Secondary parietal cortex. After Zilles (1985). Scale bar = 1 mm.

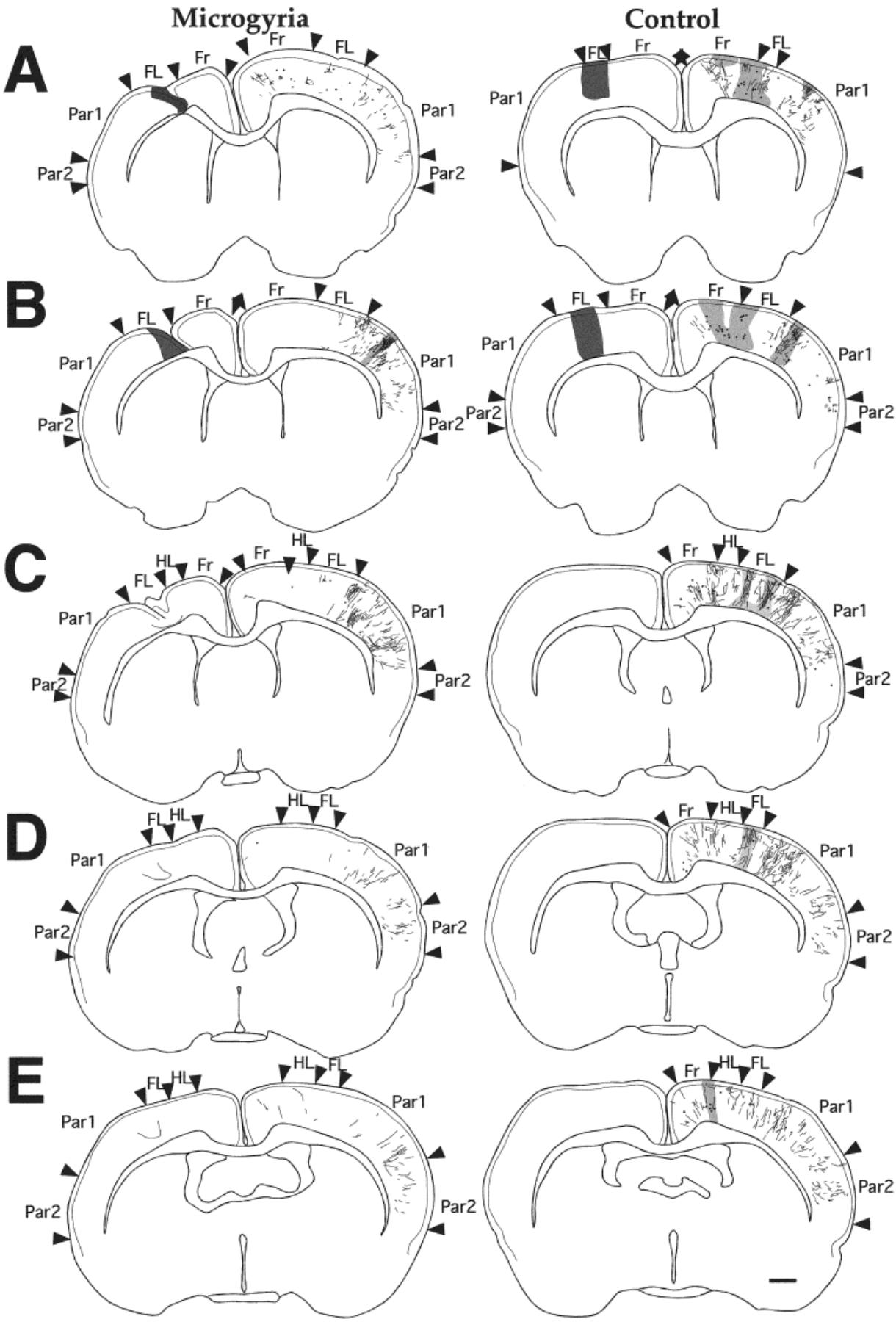

Figure 3 (Overleaf)

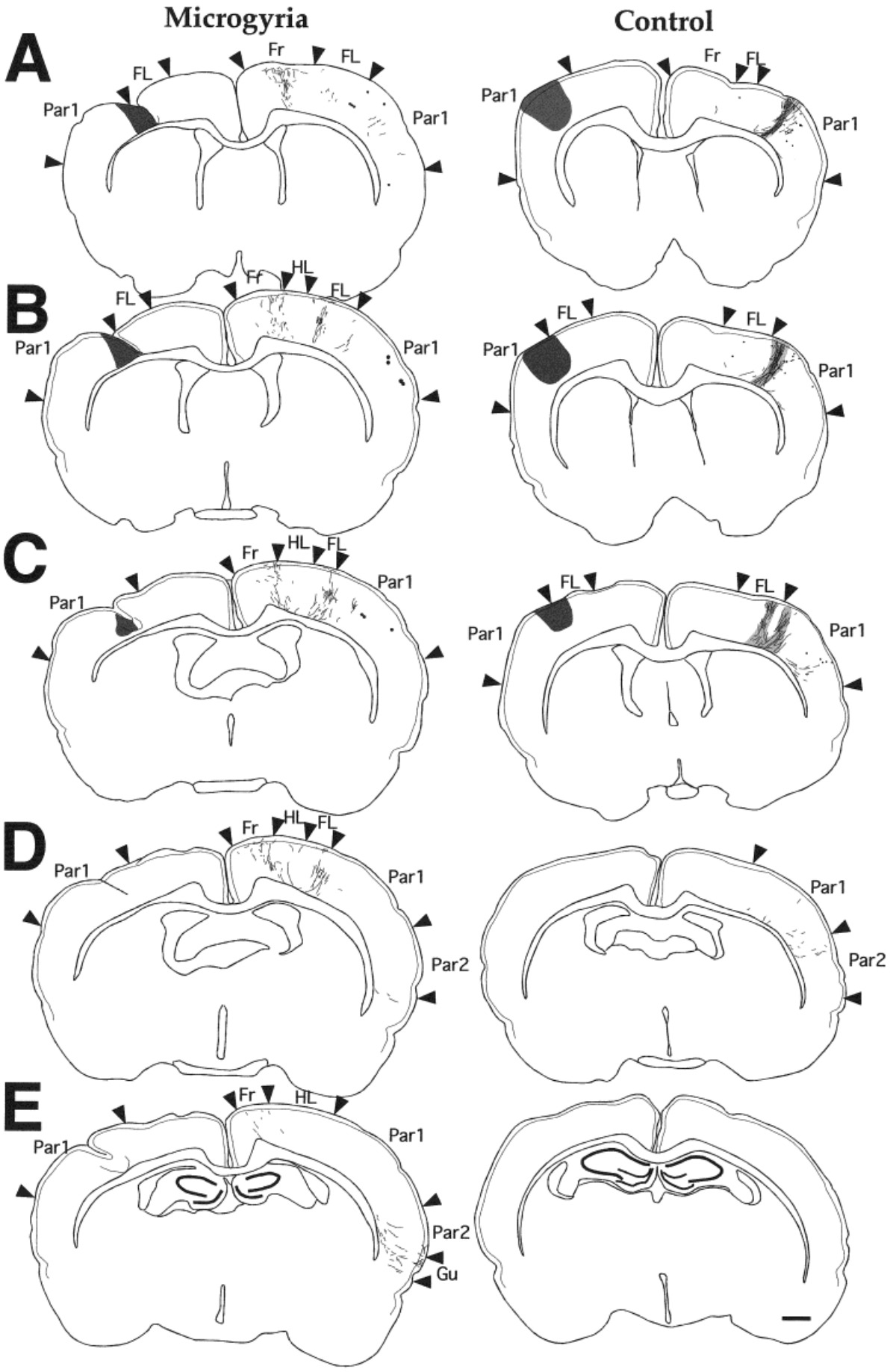

Figure 4 (Overleaf)

TABLE 2. List of Subjects and Summary of Results of Experiment 2: Injections of Tracer Into Homologous Regions of Microgyria[1]

Subject/sex	Condition	Micogyria location	Contralateral injection site	Comments
3230/M	MG	HL, FL, Par1	HL	Projections medial and lateral to MG. None in MG itself.
3231/M	Sham	—	HL	Homologous projections.
3401/M	MG	Par1, HL	Par1, HL	Projections directly into medial MG.
3402/M	Sham	—	Par1	Homologous projections, few lateral heterologous projections.
3405/M	MG	Par1	Par1	Projections into medial MG.
3406/M	Sham	—	Par1	Homologous projections.
3411/M	MG	Par1, Te	Par1	Projections into medial MG. Some projections into lateral MG. Heterologous projection to Par2/Gu border.
3416/F	MG	Par1	Par1	Projections in MG, mostly medial.
3417/F	Sham	—	Par1, HL	Homologous projections.
3419/M	Sham	—	Par1, FL	Homologous projections.
3422/F	MG	Par1, HL	Par1	Projections into MG, mostly medial MG caudally.

[1]MG, microgyria; FL, forelimb area; Fr, frontal cortex; Te, temporal cortex; Gu, gustatory cortex; HL, hindlimb area; Par1 and Par2, primary and secondary somatosensory cortices. Locations after Zilles (1985).

nearly as dense. Microgyria located in parietal cortex were virtually devoid of typical reciprocal projections with the ventrobasal complex. Thalamocortical projections at the border of the malformation were unusually dense and atypical in appearance.

We will discuss these findings in relation to what is known about the development of callosal and thalamic connections to the parietal cortex and the effects of early injury to the neocortex on connectivity. We will also speculate as to the mechanisms and consequences of connectional rearrangement.

Connectional changes following early injury

The demonstration in this study that connectivity of the brain changes following early injury is not a unique finding. In hamsters, neonatal injury to the superior colliculus resulted in altered retinal projections (Finlay et al., 1979; Schneider, 1979; Schneider, 1981). Specifically, these lesions caused optic fibers to cross the midline where they competed successfully for available terminal space in the intact superior colliculus. In monkeys, prenatal unilateral removal of portions of the frontal cortex resulted in significant displacement of callosal connections (Goldman and Galkin, 1978; Goldman-Rakic and Rakic, 1984). Removal of target regions resulted in atypical thalamic innervation (Koralek and Killackey, 1990; Schlaggar and O'Leary, 1991; O'Leary et al., 1992), and removal of the subplate regions early in development affected the development of both corticothalamic and thalamocortical projections (McConnell et al., 1989; Ghosh and Shatz, 1993; McConnell et al., 1994; Ghosh, 1995).

The above data refer to the effects of complete neonatal damage to target tissue (or to structures important to the navigation of connections to or from target tissue) on neuronal connectivity. In the present experiment, however, the entire target region was not ablated. Rather, a small focal injury caused part of the target area to be malformed, which then addresses the issue of the effects of partial injury during the perinatal period on connectivity. Miller and colleagues (1993b) demonstrated that after unilateral carotid ligation in the neonatal cat, projections to the 17/18 border from the undamaged contralateral area 17 were increased significantly. Innocenti and Berbel (1991a) demonstrated that ibotenic acid injections into the neonatal visual cortex of the cat caused a malformation resembling microgyria. They further reported that that connections to the damaged area from auditory areas AI and AII, which are normally eliminated during development, were maintained (Innocenti and Berbel, 1991b). Finally, we previously reported changes in callosal connectivity a rat case of spontaneous microgyrus (Rosen et al., 1989).

Changes in callosal connectivity

It has been known that in the parietal cortex of the adult rat, callosal projections are homotopic (Wise and Jones, 1976; Akers and Killackey, 1978). Among the controls in the current experiment, we confirmed this finding. In controls, we also found there to be some heterotopic connections, but these were much less dense than the homotopic connections and were more difficult to demonstrate. In the microgyric animals, where homotopic pro-

Fig. 4. (Overleaf) Tracing of darkfield photomontages of injection into a microgyrus located in the border between FL and Par1 of the right hemisphere of Subject 3403 (dark gray) illustrating retrograde and anterograde connections. Retrogradely labeled cells are represented as filled circles, and anterogradely labeled fibers are traced. Dense patches of projections are represented by light gray-filled regions. When compared to the matched control (Subject 3423), there is a distinct decease in density of projections to the homotopic cortical region (**A–C**). In addition, heterotopic projections to Fr (**A–E**) and Par2 and Gu (**D,E**) can be seen in the microgyric case but not in the control. Fr, Frontal cortex (including Fr1, Fr2, and Fr3); FL, Forelimb area of parietal cortex; HL, Hindlimb region of parietal cortex; Par1, Primary parietal cortex; Par2, Secondary parietal cortex; Gu, Gustatory cortex. After Zilles (1985). Scale bar = 1 mm.

Fig. 5. Afferent callosal connections to hemisphere with microgyria. **A:** Photomontage of Nissl stain of Subject 3405 showing microgyria (arrow) in Par1. Box is area of magnification for **B**. See **C** for injection site. B: High-power darkfield photomontage of BDA-stained section adjacent to A showing afferent callosal fibers to the region of the microgyrus (arrow). In this case, fibers synapse in the medial portion of the microgyrus (see Fig. 6) as well as in portions of cortex lateral to the microgyrus. C: Tracing of callosal projections from injection site (dark gray) to microgyric cortex. Dense patches of projections are represented by light gray-filled regions. **D:** Photomontage of Nissl stain of Subject 3230 showing microgyria (arrow) in Par1. Box is area of magnification for E. See F for injection site. **E:** High-power darkfield photomontage showing afferent callosal fibers to the region of the microgyrus (arrow). In this case, fibers mostly bypass the microgyrus, synapsing in regions medial and lateral to it. In addition, a small number of fibers synapse in Par2. **F:** Tracing of callosal projections from injection site (dark gray) into microgyric cortex. Fr, Frontal cortex (including Fr1, Fr2, and Fr3); FL, Forelimb region of the parietal cortex; HL, Hindlimb region of parietal cortex; Par1, Primary parietal cortex; Par2, Secondary parietal cortex. After Zilles (1985). Scale bars = 800 μm in A,C,D,F; 500 μm in B,E.

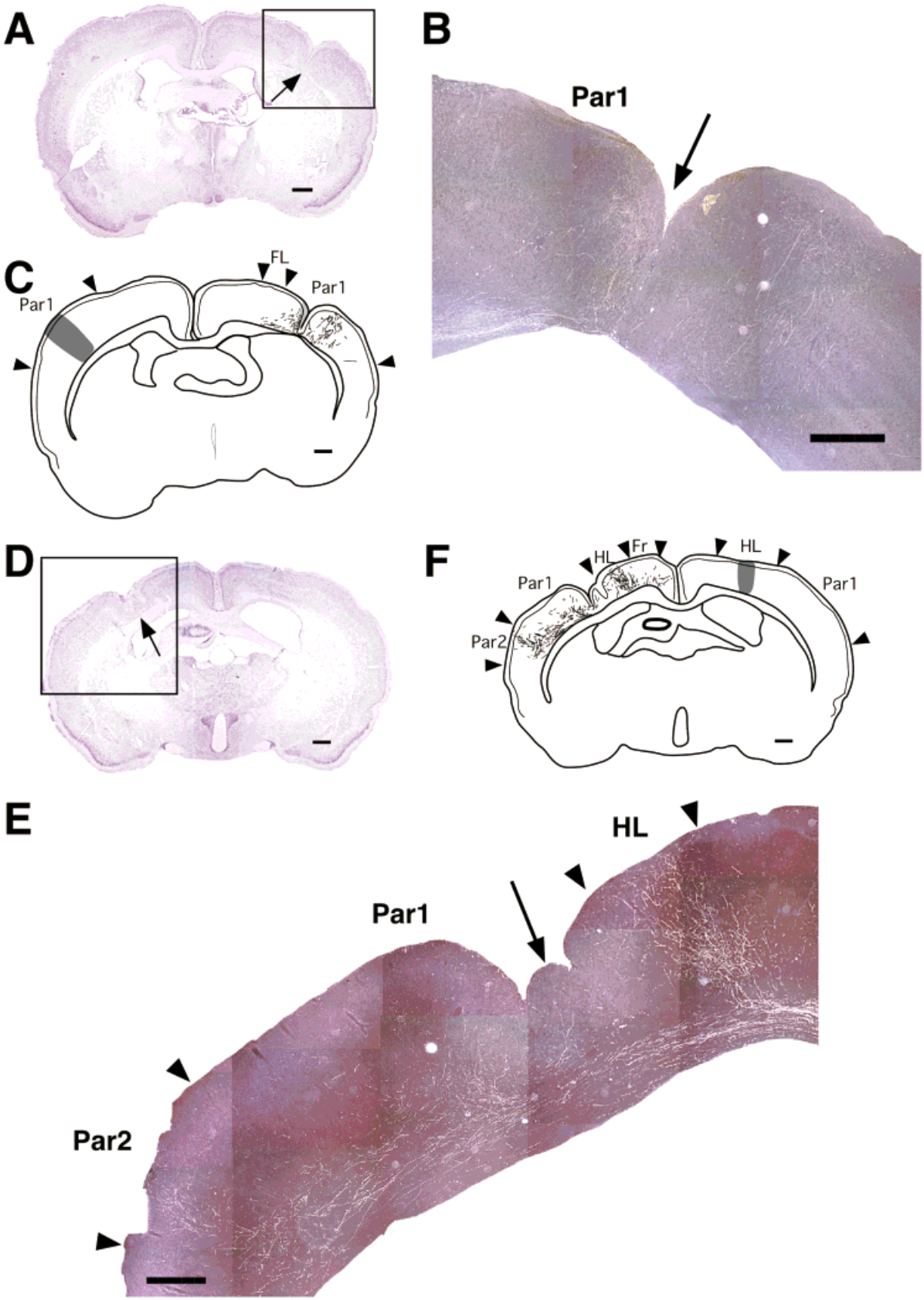

Figure 5

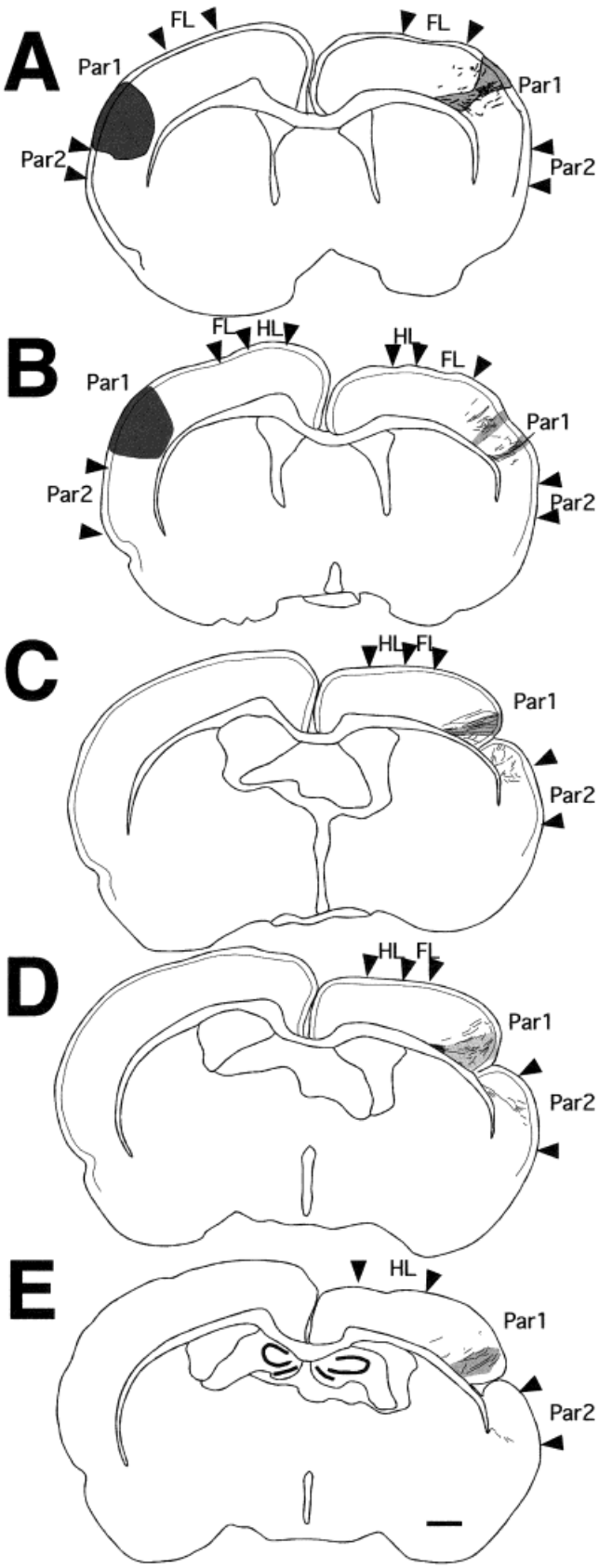

jections were seen, they were far less dense than those seen in the controls. In addition, heterotopic callosal projections in the affected animals were often found to frontal cortex and to Par2, which was never the situation in normal rats, at least not to the degree seen here. Callosal afferent projections to the microgyric region either missed the malformation entirely or were found mostly in the medial portion of it. A question can be asked regarding the way by which freezing injury to the developing cortical plate causes change in callosal connectivity. This question may best be considered in the light of what is known about the ontogenesis of callosal connections.

During early development, callosal cells of origin are distributed diffusely in the neocortex (Ivy et al., 1979; Ivy and Killackey, 1981; Innocenti and Clarke, 1984). As the brain matures, they become restricted to discrete columnar and laminar locations (Jacobson and Trojanowski, 1974; Zaborszky and Wolff, 1982). Axons from these cells cross the sagittal midline of the corpus callosum between E17 and E21 in the rat (Koester and O'Leary, 1993, 1994), after which they distribute themselves diffusely beneath the cortical plate. Finally they begin to penetrate the cortex widely, albeit not homogeneously, between P3 and P6 and reach their mature pattern sometime between the second and fourth week of life (Wise and Jones, 1976; Miller and Vogt, 1984; Olavarria and van Sluyters, 1985; Elberger, 1994). This developmental topographic restriction of callosal cells of origin and terminations is thought to result from axonal pruning rather than from the death of neurons (Ivy et al., 1979; O'Leary et al., 1981; Ivy and Killackey, 1982). It is also the case that the process of maturation of callosal connections also involves the withdrawal of transient connections (e.g., O'Leary and Stanfield, 1985; Elberger, 1994).

How might the process of injury to the developing cortical plate affect the normal developmental course of callosal connectivity? It has been previously demonstrated that the freezing injury to the brain of the newborn rat causes the formation of a microgyrus as the result of an ischemic-hypoxic insult to the developing cortical plate (Dvorák and Feit, 1977; Humphreys et al., 1991; Suzuki and Choi, 1991; Rosen et al., 1992a, 1995a). At the time of the freezing injury only the infragranular layers are present in the cortical plate (E15 and E17 birthdates), while supragranular neurons are either in the germinal zones or migrating in the intermediate zone a distance from the freezing probe (E19 and E21; Rosen et al., 1996). One day after the lesion, there is complete tissue necrosis affecting the infragranular neurons, but it appears that at least some subplate neurons survive the insult eventually to become layer iv of the microgyrus (see Fig. 1). Macro-

Fig. 6. Tracing of darkfield photomontages of BDA injection (**A,B**) into the homotopic region of the hemisphere contralateral to a microgyrus located in the border in Par1(**C–E**) of subject 3422 illustrating retrograde and anterograde connections. Retrogradely labeled cells are represented as filled circles, and anterogradely labeled fibers are traced. Dense patches of projections are represented by light gray-filled regions. Rostrally, before the obvious malformation is present (A,B), typical homotopic reciprocal projections are noted. Moving caudally (C–E), the large majority of all callosal fibers from the opposite hemisphere synapse in the medial portion of the microgyrus. A few heterotopic fibers are noted in Par2 (D,E). FL, Forelimb area of parietal cortex; HL, Hindlimb region of parietal cortex; Par1, Primary parietal cortex; Par2, Secondary parietal cortex. After Zilles (1985). Scale bar = 1 mm.

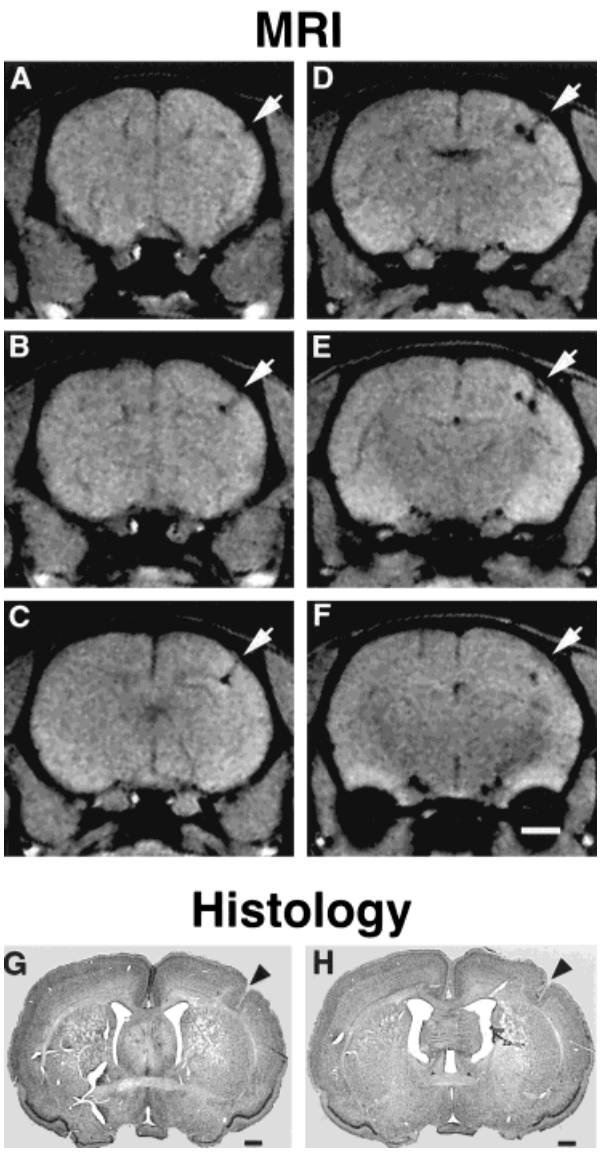

Fig. 7. Magnetic resonance gradient echo images (**A–F**) from subject 3916 and matching histology (**G,H**) illustrating location of microgyrus (arrows) in the parietal cortex of the right hemisphere. The MR images are 6 contiguous slices representing the rostral (A) to caudal (F) extent of the malformation. Images were obtained with the parameters TR/TE = 500/10 or 300/20, a FOV of 3.2 cm, with a 128 matrix (in plane resolution of 250 μm), and a section thickness of 0.5 mm. G,H: Photomicrographs of Nissl-stained sectioned from subject 3916 illustrating congruence with MR images. Scale bars = 1.5 mm in A–F; 800 μm in G,H.

phages begin to appear in excess in the damaged area and there is a dramatic increase in the number of astrocytes. Three days post-lesion, radial glial fibers regrow though a region of intense astrogliosis, and neurons again begin to migrate through that area. There is a marked increase in the number of macrophages present and the area of tissue necrosis decreases. By P7, the later born neurons destined for layer II/III finish their migration through the necrotic cortical plate and ultimately comprise layer ii of the microgyrus (Dvorák and Feit, 1977; Suzuki and Choi, 1991; Rosen et al., 1992a, 1996).

That the injury to the cortical plate and the subsequent reorganization take place at the same time that callosal fibers are beginning their innervation of the cortical plate is likely to be a key factor in the connectional changes. Thus, it could be that because nerve growth factor and other trophic factors are released during injury to nervous tissue (Nieto-Sampedro et al., 1982; Needels et al., 1986; Kromer, 1987), the heterotopic projections reflect the preservation of processes that would normally be eliminated. Furthermore, the presence of these trophic factors in the area of injury may diminish ontogenetic axonal pruning (O'Leary et al., 1981; Hamburger and Yip, 1984). The increased number of callosally-projecting neurons seen in the visual cortex of cats with carotid ligation (Miller et al., 1993b) could also reflect increased survival of developmentally transient projections (O'Leary and Terashima, 1988)—a phenomenon directly demonstrated by Innocenti and Berbel (Innocenti and Berbel, 1991b) in ibotenic-injected cats. In a related manner, other work has shown maintenance of otherwise transient projections from parietal cortex to the medial geniculate nucleus following whisker removal in rats (Nicolelis et al., 1991). Finally, it could be that the heterotopic connections are the result of increased sprouting of axodendritic processes as described in detail by Marin-Padilla (1996, 1997).

Changes in Corticothalamic and Thalamocortical Activity

Reciprocal projections between the ventrobasal complex and Par1 in normal rats have previously been demonstrated (e.g., Saporta and Kruger, 1977). Axons from the thalamus synapse mostly on neurons in layer IV, and corticothalamic projections originate predominantly in layer VI. In our microgyric animals, we found a total lack of projection either to or from the microgyric region. As stated above, the damage to the cortical plate occurs at a crucial time for the development of corticothalamic and thalamocortical projections. The question as to how early injury to the cortex might affect connectivity between the cortex and thalamus may be considered in the light of what is known about the development of connections between the thalamus and cortex.

Thalamic fibers can be seen intermingling with subplate and preplate scaffold between E15 and E16 (Catalano et al., 1996; Molnár et al., 1998). These thalamic fibers, which are also associated with early corticofugal projections (Molnár et al., 1998), appear to wait in the subplate region for 24–48 hours before invading the cortical plate itself (Catalano et al., 1991; Molnár and Blakemore, 1995). By P1, many thalamic fibers are seen within the upper portions of the cortical plate (Senft and Woolsey, 1991). They begin to elaborate their processes in layer IV of the cortex on around P4 and achieve their adult pattern soon thereafter. While the exact mechanisms are not completely understood, it is clear that axonal interactions with the subplate cells and with the cortical preplate scaffold play an important role in guiding the developing axons to their appropriate targets (Ghosh and Shatz, 1993; Molnár et al., 1998). Axons from the cortex begin to reach their thalamic targets on around P1 and achieve their mature patterns of innervation within the first week of life (Miller et al., 1993a; Frassoni et al., 1995).

The lack of cortical efferent and afferent projections in VB in the microgyric animals is not surprising. As discussed above, cells from layers IV, V, and VIa are killed during the time of the freezing injury. Because layer IV provides the targets for thalamocortical projections, and

TABLE 3. List of Subjects and Summary of Results of Experiment 3: Injections of Tracer Into Ventrobasal Complex Ipsilateral to Microgyria

Subject/sex	Condition	Micogyria location	Comments
3901/M	MG	Par1	Small projection field in Par1 appearing medial to MG. Stops at the edge of the MG.
3902/M	MG	Par1	Small projection field in Par1 appearing lateral to MG. Stops at the edge of MG.
3903/M	MG	HL, Par1	Small projection field in Par1 appears both lateral and medial to MG. Stops at edge of MG.
3904/M	MG	Par1/Par2	Projection fields in Par1 which stop at the edge of the MG. Plexus of fibers at edge of MG.
3906/M	MG	Par1	Projection field split by MG, projections on either edge. Dense bundles of fibers laterally.
3909/F	MG	HL, FL	Small injection site. Labeling very lateral and distal to medial MG. Even so, some labeled neurons go up to the border the MG.
3910/F	MG	Par1	Labeling lateral up to edge of MG
3912/M	MG	Par1	Label starts densely on lateral portion of Par1. Dense label medial to MG.
3913/M	MG	Par1, Oc	Small projection field lateral and medial to MG
3916/F	MG	Par1	Dense projection field lateral to MG. Stops at edge of MG medially and laterally. Unusually dense projections at edge of MG.
3917/F	MG	Par1	Dense projection field lateral to MG. Lesser projection field on medial edge of MG.
3918/F	MG	Par1	Dense projection field lateral to MG. Stops at edge of MG, with dense plexus of projections.
3933/F	MG	Par1, Par2	Intermittent projection fields medial to MG. Interspersed dependent upon the extent of the lesion.
3934/F	MG	HL, FL, Par1, Oc	Large but sparsely populated projection field lateral to MG. Small projection field medial to MG as well.
3935/M	Sham	—	Small projection fields in center of Par1.
3936/M	Sham	—	Projection field in center of Par1. More extensive than 3936.
3937/F	Sham	—	Large projection field in center of Par1.
3938/F	Sham	—	Dense projection field into Par1 and Par2.
3939/F	Sham	—	Projection field in center of Par1.
3941/F	Sham	—	Anterolateral layer IV and VI projection is heavy. Caudally, labeling becomes sparser.
3942/F	Sham	—	Large Par1 projection field.
3946/F	Sham	—	Heavy Par1, Par2 projection field.
3947/F	Sham	—	Heavy Par1, Par2 projection field anterolaterally.
4144/F	MG	Par1	Dense projection field lateral to MG. Plexus of fibers at lateral border of MG.
4145/F	MG	Par1, Par2	Projection field is medial to MG.
4146/F	MG	Par1, HL	Projection fields are more rostral than seen usually. Projection fields medial and lateral to MG as move caudally. Plexus of fibers at border of MG.
4148/F	MG	Par1	Projection fields deflected rostrally and medially from MG.
4149/F	MG	HL, FL, Par1	Large projection field which is most dense lateral to MG.

[1]MG, microgyria; FL, forelimb area; Fr, frontal cortex; HL, hindlimb area; Oc, occipital cortex; Par1 and Par2, primary and secondary somatosensory cortices. Locations after Zilles (1985).

layer VIa the cells of origin for corticothalamic projections, their absence in the malformation will have an obvious impact. Of greater interest are the dense patches of thalamocortical terminations that appear at the border of the microgyrus. These fibers invade layer II/III of the intact adjacent cortex and bend toward the malformed region. In area Par1, dense patterns of thalamocortical projections are associated with barrel fields, and it could be that the dense projections adjacent to the malformation are related to barrel formation. In the present study, we did not specifically assess barrel formation, but in a separate study we have seen that the majority of microgyric animals have no discernable barrels in or around malformed cortex (unpublished observations), thus making it unlikely that the dense patches have a relation to barrel fields. On the other hand, in a report based on a study using cytochrome oxidase, the authors did demonstrate the presence of barrel fields in microgyric cortex, albeit with massive distortion (Jacobs et al., 1999). Irrespective of the functional role of the dense fibers, we are interested in knowing why they orient toward the adjacent microgyrus. It may be the case that the fibers, which invade the cortex shortly after the freezing injury, are attracted to the damaged region because of the release of non-specific trophic factors, as described above. In this scenario, fibers may collect on the border of the damaged region awaiting specific signals to elaborate and innervate specific regions. Because the injured region has none of the cells that typically signal fibers to innervate are present, the fibers begin to respond to local signals and elaborated their processes at the border. Future experiments designed to trace the formation of these connections will help to definitively answer this question.

It is also important to consider the effect of freezing injury to the cortical plate on the development of the thalamus itself. We have previously shown that freezing injury to the visual cortex resulted in a diminution in volume of the lateral geniculate nucleus, although there were no changes in the size of the neurons (Herman et al., 1997). Because of the injection sites, the tissue in the current study does not lend itself to accurate determination of nuclear volume, but it is likely that the volume of VB is smaller in animals with malformations in the parietal cortex. It could therefore be the case that one explanation for our results is that there are fewer cells in VB of microgyric animals. We do not view this as likely, as the key feature in our results is an *absence* of labeled fibers and cells locally in the malformation—the borders of the microgyrus, which are also in parietal cortex, have intact projections.

Evidence of widespread changes due to the malformation

The results of the present experiment suggest that developmental focal and partial injury to the cortical plate, which results in a disturbance in neuronal migration, can have widespread changes throughout the forebrain. This claim is bolstered by previous reports noting that the severity and extent of the malformation is not always apparent from the examination of Nissl-stained material. Glutamatergic neurons, for example, which are altogether absent from the microgyrus, are also disturbed in regions surrounding the microgyrus (Humphreys et al., 1991). Moreover, Zilles (1998) found up-regulation of excitatory receptors (NMDA, Kainate, AMPA) and down-regulation of $GABA_A$ and $GABA_B$ receptors in microgyria, as well as AMPA- and Kainate-receptor up-regulation and $GABA_A$ down-regulation in regions adjacent to the microgyrus of adult rats. We, too, showed that the number of parvalbumin-immunoreactive neurons, which are mainly

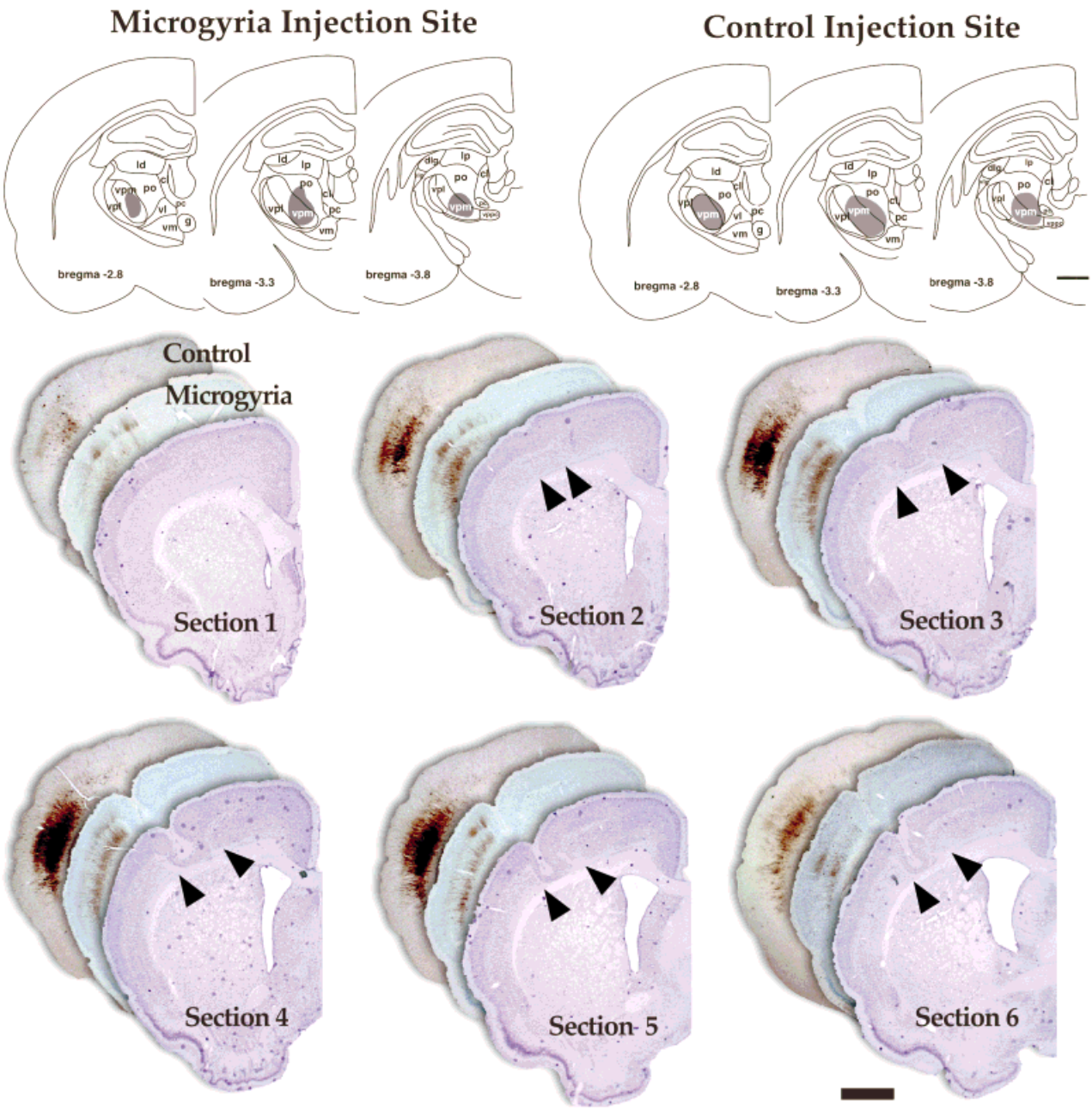

Fig. 8. Thalamocortical and corticothalamic projections between VB and Par1 in microgyric and control rats. **Top:** Injection sites of BDA targeted to the VB of microgyric (Subject 4144) and control (Subject 3946) rats. **Bottom:** A series of six photomicrographic montages. Frontmost section is a Nissl-stained section from microgyric subject. Directly beneath this Nissl section is an adjacent section stained for BDA. The bottommost section is from the control subject and is matched to those from the microgyric animal. Arrowheads on the Nissl-stained sections denote the microgyrus. Note the general decrease in the density of projection in the microgyric subject, and the complete absence of thalamocortical or corticothalamic projections in the microgyric region. cl, centrolateral n.; dlg, dorsal lateral geniculate n., ld, laterodorsal n.; lp, lateral posterior n.; pc, paracentral n.; po, posterior n.; vlg, ventral lateral geniculate n.; vm, ventromedial n.; vpl, ventroposterior n.; vpm, ventromedial n.; vppc, ventroposterior, parvocellular n. Nuclei after Paxinos and Watson (1986). Scale bars = 1 mm in top panel; 1.5 mm in bottom panel.

GABAergic, are decreased early on both within and outside the microgyrus, (Rosen et al., 1998).

Furthermore, recent evidence indicates that electrical stimulation of cortical neurons lying outside the microgyrus results in epileptogenic discharges that can be recorded as far away as 3–4 mm from the site of stimulation (Jacobs et al., 1996; Luhmann et al., 1997, 1998). It is interesting to note that the dense plexus of thalamocortical fibers located at the border of the microgyrus is precisely the place where stimulation induces epileptiform discharges. It is tempting to speculate that the thalamocortical axons in this region facilitate the epileptogenic activity of the neurons present at that site, but there is no direct evidence as yet to link the two.

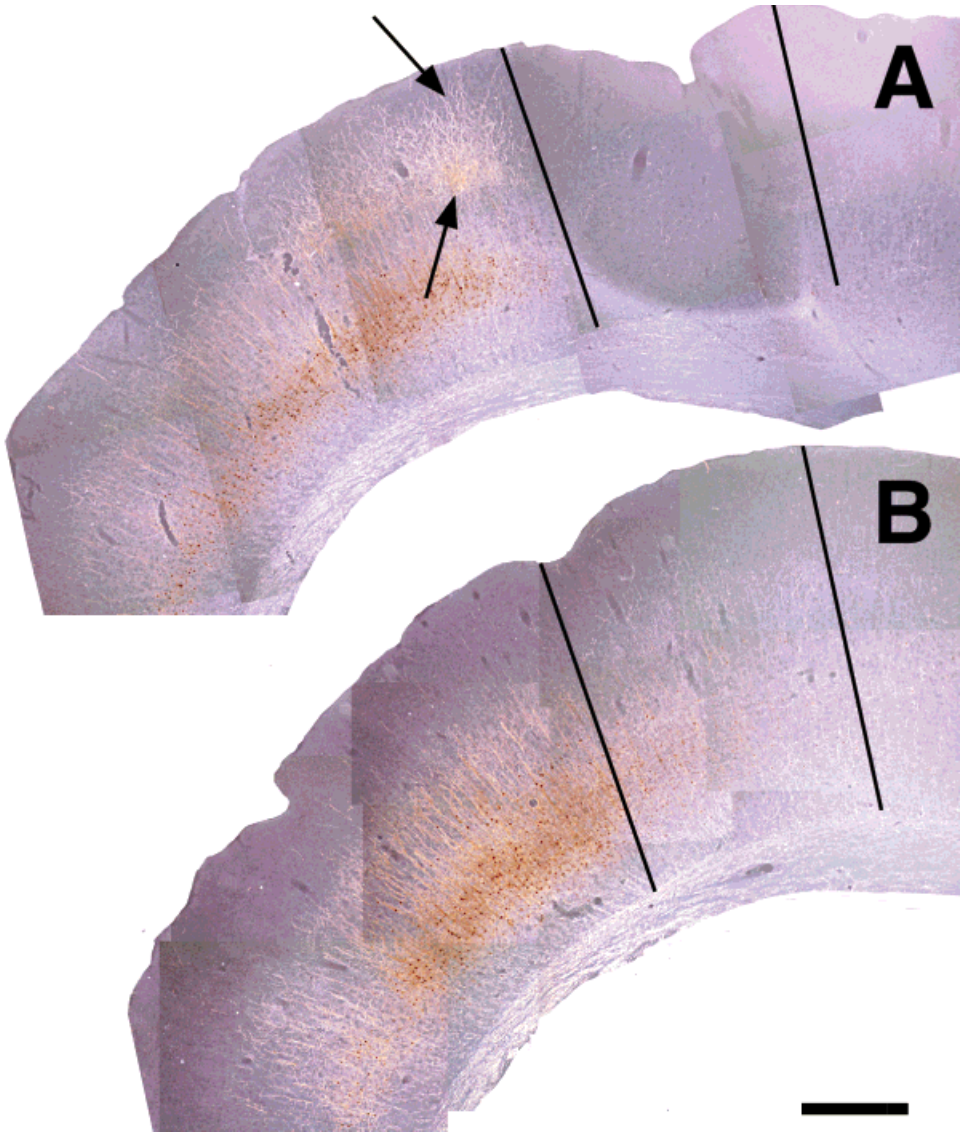

Fig. 9. **A:** High-power darkfield photomontage showing thalamocortical (fibers) and corticothalamic (dark cells in layer VI) projections from Subject 4144 (section 3 from Fig. 8). Arrows indicate dense patch of thalamocortical fibers in layer II/III of the cortex at the border of the microgyric region. Lines denote microgyric region. Note lack of projections in the microgyric region itself. **B:** High-power darkfield photomontage showing thalamocortical (fibers) and corticothalamic (dark cells in layer VI) projections from control Subject 3946. Note increase of efferent and afferent projections in the region homologous to the microgyria (lines). Scale bar = 500 μm.

One question that is not addressed by the current experiments is whether the microgyric region connects with thalamic nuclei with which normal cortex does not. In Experiment 1, we placed injections directly into the microgyrus for the primary purpose of examining efferent callosal connections. Examination of the thalamus of these animals revealed a marked paucity of fibers or retrogradely labeled cells. When labeling was present, it was always in thalamic nuclei appropriate for the regions of injection (VB or Po predominantly), albeit quite diminished when compared to controls. We did not see evidence of extraneous projections. Future experiments designed to describe the formation of these connections will help to completely address this question.

Disorders of neuronal migration and connectivity

Evidence from the literature suggests that despite sometimes gross changes in neuronal migration to the neocortex, the intrinsic patterns of connectivity are not generally disturbed. Efferent connections in the cortex of the reeler mouse are relatively normal despite the inversion of the laminar structure of the cortex (Caviness, 1976, 1982; Caviness and Yorke, 1976; Caviness and Frost, 1983; Goffinet et al., 1984; Frost et al., 1986). The subcortical heterotopic collection of neurons that characterize the *tish* model of double cortex also appear to have connections typical of neocortical neurons (Schottler et al.,

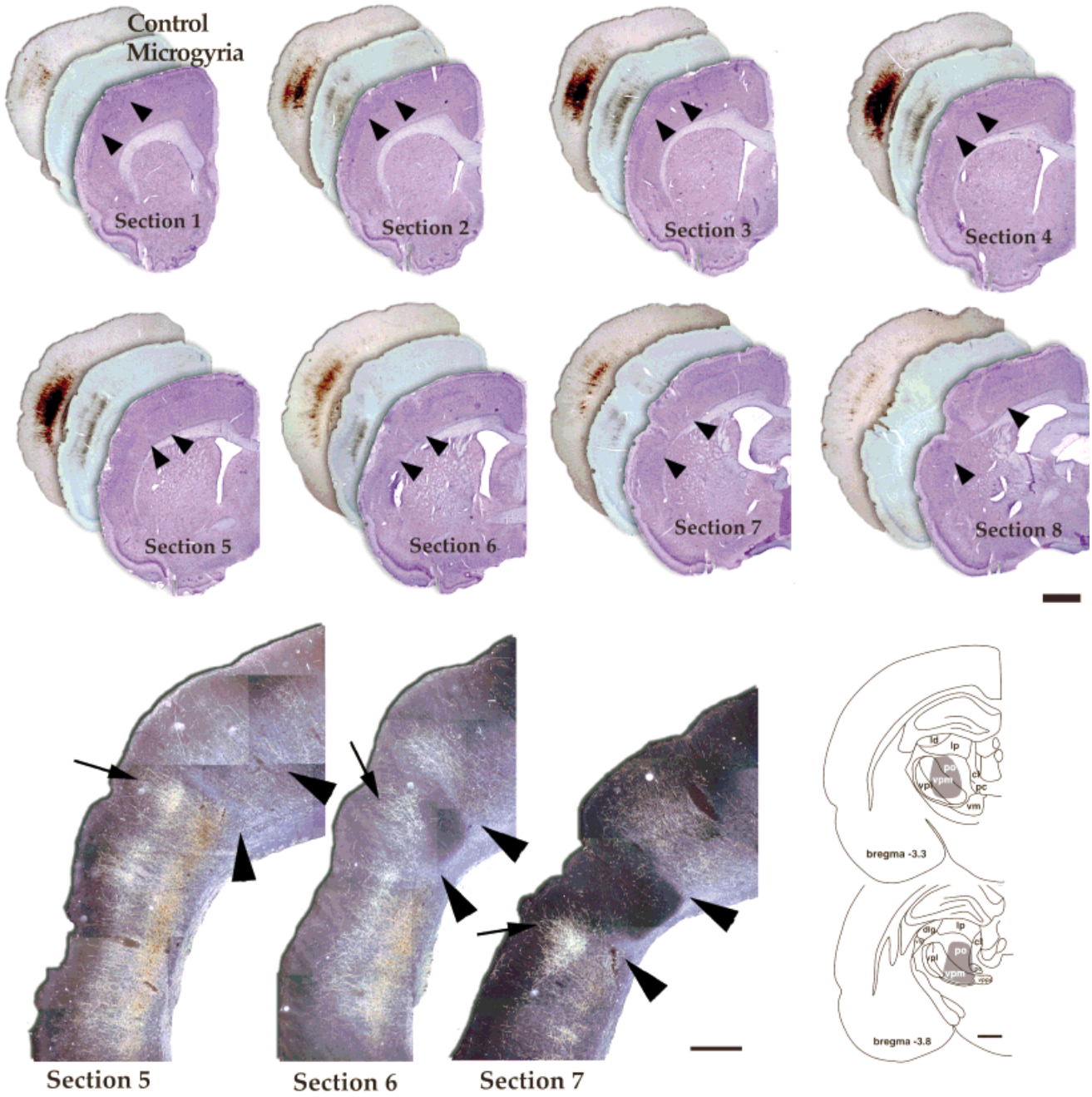

Fig. 10. Thalamocortical and corticothalamic projections between VB and Par1 in microgyric and control rats. **Top:** A series of six photomicrographic montages. Frontmost section is a Nissl-stained section from Subject 4146. Directly beneath this Nissl section is an adjacent section stained for BDA. The bottom-most section is from the same control subject as see in Figure 8 and is matched to those from the microgyric animal. Arrowheads on the Nissl-stained sections denote the microgyrus. As with Figure 8, note the general decrease in the density of projection in the microgyric subject and the relative absence of thalamocortical or corticothalamic projections in the microgyric region. Note also projections both lateral and medial to Sections 7 and 8, which reflect the position of this microgyrus in the middle of the projection field for VB. **Bottom Left:** Darkfield photomontages showing thalamocortical (fibers) and corticothalamic (dark cells in layer VI) projections in Sections 5, 6, and 7 at higher magnification. Arrows denote dense plexus of thalamocortical fibers at the border of the microgyric region, especially in Section 7. Also note the paucity of projections in the microgyric region itself. **Bottom Right:** Injection site of BDA targeted to the VB of microgyric Subject 4146. For abbreviations, see Figure 8. Scale bars = 1.5 mm in top panel; 500 μm in bottom left; 1 mm in bottom right.

1998). Finally, the ectopic collection of neurons in CA1 of the hippocampus of MAM-injected animals appear to have connections that are appropriate for their ontogenetic origin (neocortical). In addition, they also have connections appropriate for their new location (Chevassus-Au-Louis et al., 1998b,c).

We report here that efferent and afferent connections can change following induction of a malformation. It is likely that the key difference between the previous reports and our own lies in the mechanism underlying the migrational disorder. In our case, we induce a malformation resembling human microgyria by a focal injury to the developing cortical plate. In contrast, there is no evidence of direct injury to the neocortex causing these other migrational disturbances. Rather, these migrational disorders are most probably the result of a disruption in the signals important to orderly migration of neurons to the cortex (D'Arcangelo et al., 1995, 1997; Lee et al., 1997, 1998; Chevassus-Au-Louis et al., 1998b,c). We hypothesize, therefore, that *both* the connectional changes and the microgyria-like malformation are the result of injury to the developing cortical plate rather than the latter directly affecting the former.

Conclusions

Freezing injury to the cortical plate induces a malformation resembling human cerebral microgyria. Despite the focal nature of these anomalies, widespread effects on distant anatomy, physiology and behavior have been noted. We had previously hypothesized that one possibility to explain these far-reaching disturbances would be through the demonstration of changes in the connectivity associated with injury to the cortical plate. In the current experiments, we have demonstrated changes in callosal, thalamocortical, and corticothalamic connections associated with induced microgyria. Specifically, we report an increase in heterotopic as well as an absence of homotopic callosal projections. There are few or no thalamocortical or corticothalamic connections between parietal microgyria and ventrobasal complex. A dense zone of thalamocortical terminations is seen at the border of the malformation that could underlie, at least in part, the neurophysiologic disturbances. Taken as a whole, these data support the notion that widespread changes in the cortical and subcortical cellular and connectional architecture can arise from focal injury occurring during critical periods of cortical development.

Note added in proof. A recent report has also examined callosal connectivity in microgyric rats (Giannetti et al., 1999). In this study, the authors induced microgyria into the frontal cortex of the left hemisphere and, in adulthood, injected HRP into the contralateral homologous cortex. They found few retrogradely-labeled cells in the microgyrus itself, but did find large numbers of retrogradely-labeled cells in the region immediately lateral to the microgyrus. Moreover, they found that the radial alignment and pattern of laminar distribution of these cells differed from that of controls. This study differs from the present study in the location of the induced malformation (frontal vs. parietal) and the type of labeling associated with the neuronal tracer (primarily retrograde vs. primarily anterograde). That being said, it is interesting to note that it is the region adjacent to the microgyrus that displays aberrant patterns of connectivity—a finding similar to what we report with thalamocortical and callosal projections to microgyric parietal cortex.

ACKNOWLEDGMENTS

The authors thank Heinz Windzio, Aaron Levine, and Dr. Jeeva Munasinghe for their technical assistance.

LITERATURE CITED

Akers RM, Killackey HP. 1978. Organization of corticocortical connections in the parietal cortex of the rat. J Comp Neurol 181:513–538.

Baraban SC, Schwartzkroin PA. 1996. Flurothyl seizure susceptibility in rats following prenatal methylazoxymethanol treatment. Epilepsy Res 23:189–194.

Catalano SM, Robertson RT, Killackey HP. 1991. Early ingrowth of thalamocortical afferents to the neocortex of the prenatal rat. Proc Natl Acad Sci USA 88:2999–3003.

Catalano SM, Robertson RT, Killackey HP. 1996. Individual axon morphology and thalamocortical topography in developing rat somatosensory cortex. J Comp Neurol 367:36–53.

Caviness VS, Jr. 1976. Patterns of cell and fiber distribution in the neocortex of the reeler mutant mouse. J Comp Neurol 170:435–448.

Caviness VS, Jr. 1982. Neocortical histogenesis and reeler mice: a developmental study based upon [^{3}H]thymidine autoradiography. Brain Res Dev Brain Res 4:293–302.

Caviness VS, Jr., Frost DO. 1983. Thalamocortical projections in the reeler mutant mouse. J Comp Neurol 219:182–202.

Caviness VS, Jr., Yorke CH, Jr. 1976. Interhemispheric neocortical connections of the corpus callosum in the reeler mutant mouse: a study based on anterograde and retrograde methods. J Comp Neurol 170: 449–460.

Chevassus-au-Louis N, Ben-Ari Y, Vergnes M. 1998a. Decreased seizure threshold and more rapid rate of kindling in rats with cortical malformation induced by prenatal treatment with methylazoxymethanol. Brain Res 812:252–255.

Chevassus-Au-Louis N, Congar P, Represa A, Ben-Ari Y, Gaiarsa JL. 1998b. Neuronal migration disorders: heterotopic neocortical neurons in CA1 provide a bridge between the hippocampus and the neocortex. Proc Natl Acad Sci USA 95:10263–10268.

Chevassus-Au-Louis N, Rafiki A, Jorquera I, Ben-Ari Y, Represa A. 1998c. Neocortex in the hippocampus: an anatomical and functional study of CA1 heterotopias after prenatal treatment with methylazoxymethanol in rats. J Comp Neurol 394:520–536.

Dambska M, Haddad R, Kozlowski PB, Lee MH, Shek J. 1982. Telencephalic cytoarchitectonics in the brains of rats with graded degrees of micrencephaly. Acta Neuropathol 58:203–209.

D'Arcangelo, Miao G, Chen C, Soares H, Morgan I, Curran T. 1995. Protein related to extracellular-matrix proteins deleted: the mouse mutant reeler. Nature 374:719–723.

D'Arcangelo G, Nakajima K, Miyata T, Ogawa M, Mikoshiba K, Curran T. 1997. Reelin is a secreted glycoprotein recognized by the CR-50 monoclonal antibody. J Neurosci 17:23–31.

Dvorák K, Feit J. 1977. Migration of neuroblasts through partial necrosis of the cerebral cortex in newborn rats: contribution to the problems of morphological development and developmental period of cerebral microgyria. Acta Neuropathol (Berl) 38:203–212.

Dvorák K, Feit J, Juránková Z. 1978. Experimentally induced focal microgyria and status verrucosus deformis in rats: pathogenesis and interrelation histological and autoradiographical study. Acta Neuropathol Berlin 44:121–129.

Elberger AJ. 1994. Transitory corpus callosum axons projecting throughout developing rat visual cortex revealed by diI. Cereb Cortex 4:279–299.

Finlay BL, Wilson KG, Schneider GE. 1979. Anomalous ipsilateral retinotectal projections in Syrian hamsters with early lesions: topography and functional capacity. J Comp Neurol 183:721–740.

Fitch RH, Brown CP, Tallal P, Rosen GD. 1997. Effects of sex and MK-801 on auditory-processing deficits associated with developmental microgyric lesions in rats. Behav Neurosci 111:404–412.

Fitch RH, Tallal P, Brown C, Galaburda AM, Rosen GD. 1994. Induced microgyria and auditory temporal processing in rats: a model for language impairment? Cereb Cortex 4:260–270.

Frassoni C, Arcelli P, Regondi MC, Selvaggio M, Debiasi S, Spreafico R. 1995. Branching pattern of corticothalamic projections from the somatosensory cortex during postnatal development in the rat. Brain Res Dev Brain Res 90:111–121.

Frost DO, Edwards MA, Sachs GM, Caviness VS, Jr. 1986. Retinotectal projection in reeler mutant mice: relationships among axon trajectories, arborization patterns and cytoarchitecture. Dev Brain Res 28: 109–120.

Ghosh A. 1995. Subplate neurons and the patterning of thalamocortical

connections. In: Bock G, Cardew G, editors. Development of the cerebral cortex. New York: John Wiley and Sons. p 150–172.

Ghosh A, Shatz CJ. 1993. A role for subplate neurons in the patterning of connections from thalamus to neocortex. Development 117:1031–1047.

Giannetti S, Gaglini P, Granato A, Di Rocco C. 1999. Organization of callosal connections in rats with experimentally induced microgyria. Childs Nerv Syst 15:444–448.

Goffinet AM, So K-F, Yamamoto M, Edwards M, Caviness VS, Jr. 1984. Architectonic and hodological organization of the cerebellum in reeler mutant mice. Brain Res Dev Brain Res 16:263–276.

Goldman PS, Galkin TW. 1978. Prenatal removal of frontal association cortex in the fetal rhesus monkey: anatomical and functional consequences in postnatal life. Brain Res 152:451–485.

Goldman-Rakic PS, Rakic P. 1984. Experimentally modified convolutional patterns in nonhuman primates: Possible relevance of connections to cerebral dominance in humans. In: Geschwind N, Galaburda AM, editors. Biological foundations of cerebral dominance. Cambridge, Massachusetts: Harvard University Press. p 179–192.

Hamburger V, Yip JW. 1984. Reduction of experimentally induced neuronal death in spinal ganglia of the chick embryo by nerve growth factor. J Neurosci 4:764–774.

Herman AE, Galaburda AM, Fitch HR, Carter AR, Rosen GD. 1997. Cerebral microgyria, thalamic cell size and auditory temporal processing in male and female rats. Cereb Cortex 7:453–464.

Humphreys P, Rosen GD, Press DM, Sherman GF, Galaburda AM. 1991. Freezing lesions of the newborn rat brain: a model for cerebrocortical microgyria. J Neuropathol Exp Neurol 50:145–160.

Innocenti GM, Berbel P. 1991a. Analysis of an experimental cortical network: i) architectonics of visual areas 17 and 18 after neonatal injections of ibotenic acid; similarities with human microgyria. J Neur Transplant 2:1–28.

Innocenti GM, Berbel P. 1991b. Analysis of an experimental cortical network: ii) Connections of visual areas 17 and 18 after neonatal injections of ibotenic acid. J Neur Transplant 2:29–54.

Innocenti GM, Clarke S. 1984. The organization of immature callosal connections. J Comp Neurol 230:287–309.

Ivy GO, Akers RM, Killackey HP. 1979. Differential distribution of callosal projections in the neonatal and adult rat. Brain Res 173: 532–537.

Ivy GO, Killackey HP. 1981. The ontogeny of the distribution of callosal projection neurons in the rat parietal cortex. J Comp Neurol 195:367–389.

Ivy GO, Killackey HP. 1982. Ontogenetic changes in the projections of neocortical neurons. J Neurosci 2:735–743.

Jacobs K, Mogensen M, Warren E, Prince D. 1999. Experimental microgyri disrupt the barrel field pattern in rat somatosensory cortex. Cereb Cortex 9:733–744.

Jacobs KM, Gutnick MJ, Prince DA. 1996. Hyperexcitability in a model of cortical maldevelopment. Cereb Cortex 6:514–523.

Jacobs KM, Mogensen M, Warren L, Prince DA. 1997. Experimental microgyri disrupt cytochrome oxidase-identified barrel formation in rat somatosensory cortex. Soc Neurosci Abstr 23:811.

Jacobson S, Trojanowski JQ. 1974. The cells of origin of the corpus callosum in the rat, cat and rhesus monkey. Brain Res 74:149–155.

Johnston MV, Coyle JT. 1979. Histological and neurochemical effects of fetal treatment with methylazoxymethanol on rat neocortex in adulthood. Brain Res 170:135–155.

Koester SE, O'Leary DD. 1993. Connectional distinction between callosal and subcortically projecting cortical neurons is determined prior to axon extension. Dev Biol 160:1–14.

Koester SE, O'Leary DD. 1994. Axons of early generated neurons in cingulate cortex pioneer the corpus callosum. J Neurosci 14:6608–6620.

Koralek KA, Killackey HP. 1990. Callosal projections in rat somatosensory cortex are altered by early removal of afferent input. Proc Natl Acad Sci USA 87:1396–1400.

Kromer LF. 1987. Nerve growth factor treatment after brain injury prevents neuronal death. Science 235:214–216.

Lee KS, Collins JL, Anzivino MJ, Frankel EA, Schottler F. 1998. Heterotopic neurogenesis in a rat with cortical heterotopia. J Neurosci 18: 9365–9375.

Lee KS, Schottler F, Collins JL, Lanzino G, Couture D, Rao A, Hiramatsu K, Goto Y, Hong SC, Caner H, Yamamoto H, Chen ZF, Bertram E, Berr S, Omary R, Scrable H, Jackson T, Goble J, Eisenman L. 1997. A genetic animal model of human neocortical heterotopia associated with seizures. J Neurosci 17:6236–6242.

Luhmann HJ, Karpuk N, Qü M, Zilles K. 1997. Neuronal migration disorders in rat cerebral cortex: Electrophysiological and anatomical characterization. Soc Neurosci Abstr 23:807.

Luhmann HJ, Raabe K. 1996. Characterization of neuronal migration disorders in neocortical structures. 1. Expression of epileptiform activity in an animal model. Epilepsy Res 26:67–74.

Luhmann HJ, Raabe K, Qü M, Zilles K. 1998. Characterization of neuronal migration disorders in neocortical structures: extracellular in vitro recordings. Eur J Neurosci 10:3085–3094.

Marin-Padilla M. 1996. Developmental neuropathology and impact of perinatal brain damage. I. hemorrhagic lesions of neocortex. J Neuropathol Exp Neurol 55:758–773.

Marin-Padilla M. 1997. Developmental neuropathology and impact of perinatal brain damage. II: white matter lesions of the neocortex. J Neuropathol Exp Neurol 56:219–235.

McConnell SK, Ghosh A, Shatz CJ. 1989. Subplate neurons pioneer the first axon pathway from the cerebral cortex. Science 245:978–982.

McConnell SK, Ghosh A, Shatz CJ. 1994. Subplate pioneers and the formation of descending connections from cerebral cortex. J Neurosci 14:1892–1907.

Miller B, Chou L, Finlay BL. 1993a. The early development of thalamocortical and corticothalamic projections. J Comp Neurol 335:16–41.

Miller B, Nagy D, Finlay BL, Chance B, Kobayashi A, Nioka S. 1993b. Consequences of reduced cerebral blood flow in brain development. I. Gross morphology, histology, and callosal connectivity. Exp Neurol 124:326–342.

Miller MW, Vogt BA. 1984. The postnatal growth of the callosal connections of primary and secondary visual cortex in the rats. Brain Res Dev Brain Res 14:304–309.

Molnár Z, Adams R, Blakemore C. 1998. Mechanisms underlying the early establishment of thalamocortical connections in the rat. J Neurosci 18:5723–5745.

Molnár Z, Blakemore C. 1995. How do thalamic axons find their way to the cortex? Trends Neurosci 18:389–397.

Needels DL, Nieto-Sampedro M, Cotman CW. 1986. Induction of a neurite-promoting factor in rat brain following injury or deafferentiation. Neuroscience 18:517–526.

Nicolelis MAL, Chapin JK, Lin RCS. 1991. Neonatal whisker removal in rats stabilizes a transient projection from the auditory thalamus to the primary somatosensory cortex. Brain Res 567:133–139.

Nieto-Sampedro M, Lewis ER, Cotman CW, Manthorpe M, Staper SD, Barbin G, Longo FM, Varon S. 1982. Brain injury causes a time-dependent increase in neuronotrophic activity at the lesion site. Science 217:860–861.

O'Leary DDM, Schlaggar BL, Stanfield BB. 1992. The specification of sensory cortex: Lessons from cortical transplantation. Exp Neurol 115: 121–126.

O'Leary DDM, Stanfield BB. 1985. Occipital cortical neurons with transient pyramidal tract axons extend and maintain collaterals to subcortical but not intacortical targets. Brain Res 336:326–333.

O'Leary DDM, Stanfield BB, Cowan WM. 1981. Evidence that the early postnatal restriction of the cells of origin of the callosal projection is due to the elimination of axonal collaterals rather than to the death of neurons. Brain Res 227:607–617.

O'Leary DDM, Terashima T. 1988. Cortical axons branch to multiple subcortical targets by interstitial axon budding: Implications for target recognition and "waiting periods." Neuron 1:901–910.

Olavarria J, van Sluyters RC. 1985. Organization and postnatal development of callosal connections in the visual cortex of the rat. J Comp Neurol 239:1–26.

Paxinos G, Watson C. 1986. The rat brain in stereotaxic coordinates. Sydney; Orlando: Academic Press.

Rafiki A, Chevassus-au-Louis N, Ben-Ari Y, Khrestchatisky M, Represa A. 1998. Glutamate receptors in dysplasic cortex: an in situ hybridization and immunohistochemistry study in rats with prenatal treatment with methylazoxymethanol. Brain Res 782:142–152.

Rosen GD, Burstein D. 1997. MRI visualization of focal induced neocortical malformations of the rat. Neuroreport 8:3883–3887.

Rosen GD, Galaburda AM, Sherman GF. 1989. Cerebrocortical microdysgenesis with anomalous callosal connections: a case study in the rat. Int J Neurosci 47:237–247.

Rosen GD, Herman AE, Galaburda AM. 1997. MGN neuronal size distribution following induced neocortical malformations: the effect of perinatal gonadal steroids. Soc Neurosci Abstr 23:626.

Rosen GD, Herman AE, Galaburda AM. 1999. Sex differences in the effects of early neocortical injury on neuronal size distribution of the medial geniculate nucleus in the rat are mediated by perinatal gonadal steroid. Cereb Cortex 9:27–34.

Rosen GD, Jacobs KM, Prince DA. 1998. Effects of neonatal freeze lesions on expression of parvalbumin in rat neocortex. Cereb Cortex 8:753–761.

Rosen GD, Press DM, Sherman GF, Galaburda AM. 1992a. The development of induced cerebrocortical microgyria in the rat. J Neuropathol Exp Neurol 51:601–611.

Rosen GD, Richman JM, Sherman GF, Galaburda AM. 1992b. Birthdates of neocortical neurons in induced microgyria in the rat. Soc Neurosci Abstr 18:1446.

Rosen GD, Sherman GF, Galaburda AM. 1994. Radial glia in the neocortex of adult rats: effects of neonatal brain injury. Brain Res Dev Brain Res 82:127–135.

Rosen GD, Sherman GF, Galaburda AM. 1996. Birthdates of neurons in induced microgyria. Brain Res 727:71–78.

Rosen GD, Sigel EA, Sherman GF, Galaburda AM. 1995a. The neuroprotective effects of MK-801 on the induction of microgyria by freezing injury to the newborn rat neocortex. Neuroscience 69:107–114.

Rosen GD, Waters NS, Galaburda AM, Denenberg VH. 1995b. Behavioral consequences of neonatal injury of the neocortex. Brain Res 681:177–189.

Saporta S, Kruger L. 1977. The organization of thalamocortical relay neurons in the rat ventrobasal complex studied by the retrograde transport of horseradish peroxidase. J Comp Neurol 174:187–208.

Schlaggar BL, O'Leary DDM. 1991. Potential of visual cortex to develop an array of functional units unique to somatosensory cortex. Science 252: 1556–1560.

Schneider GE. 1979. Is it really better to have your brain lesion early? A revision of the "Kennard principle." Neuropsychologia 17:557–583.

Schneider GE. 1981. Early lesions and abnormal neuronal connections. Trends Neurosci 4:187–192.

Schottler F, Couture D, Rao A, Kahn H, Lee KS. 1998. Subcortical connections of normotopic and heterotopic neurons in sensory and motor cortices of the *tish* mutant rat. J Comp Neurol 395:29–42.

Senft SL, Woolsey TA. 1991. Growth of thalamic afferents into mouse barrel cortex. Cereb Cortex 1:308–335.

Singh SC. 1977. Ectopic neurones in the hippocampus of the postnatal rat exposed to methylazoxymethanol during foetal development. Acta Neuropathol (Berl) 40:111–116.

Suzuki M, Choi BH. 1991. Repair and reconstruction of the cortical plate following closed cryogenic injury to the neonatal rat cerebrum. Acta Neuropathol Berlin 82:93–101.

Wise SP, Jones EG. 1976. The organization and postnatal development of the commissural projection of the rat somatic sensory cortex. J Comp Neurol 168:313–343.

Zaborszky L, Wolff JR. 1982. Distributional patterns and individual variations of callosal connections in the albino rat. Anat Embryol 165:213–232.

Zilles K. 1985. The cortex of the rat: a stereotaxic atlas. Berlin: Springer-Verlag.

Zilles K, Qü M, Schleicher A, Luhmann HJ. 1998. Characterization of neuronal migration disorders in neocortical structures: quantitative receptor autoradiography of ionotropic glutamate, GABA(A) and GABA(B) receptors. Eur J Neurosci 10:3095–3106.